

Accepted Manuscript

Self-assembly, AIEE and mechanochromic properties of amphiphilic α -cyanostilbene derivatives

Yanming Ren, Ruilin Zhang, Chao Yan, Tingyan Wang, Huifang Cheng, Xiaohong Cheng



PII: S0040-4020(17)30727-5

DOI: [10.1016/j.tet.2017.07.010](https://doi.org/10.1016/j.tet.2017.07.010)

Reference: TET 28842

To appear in: *Tetrahedron*

Received Date: 19 May 2017

Revised Date: 3 July 2017

Accepted Date: 7 July 2017

Please cite this article as: Ren Y, Zhang R, Yan C, Wang T, Cheng H, Cheng X, Self-assembly, AIEE and mechanochromic properties of amphiphilic α -cyanostilbene derivatives, *Tetrahedron* (2017), doi: 10.1016/j.tet.2017.07.010.

This is a PDF file of an unedited manuscript that has been accepted for publication. As a service to our customers we are providing this early version of the manuscript. The manuscript will undergo copyediting, typesetting, and review of the resulting proof before it is published in its final form. Please note that during the production process errors may be discovered which could affect the content, and all legal disclaimers that apply to the journal pertain.

Graphical Abstract

Self assembly, AIEE and mechanochromic properties of amphiphilic α -cyanostilbene derivatives

Leave this area blank for abstract info.

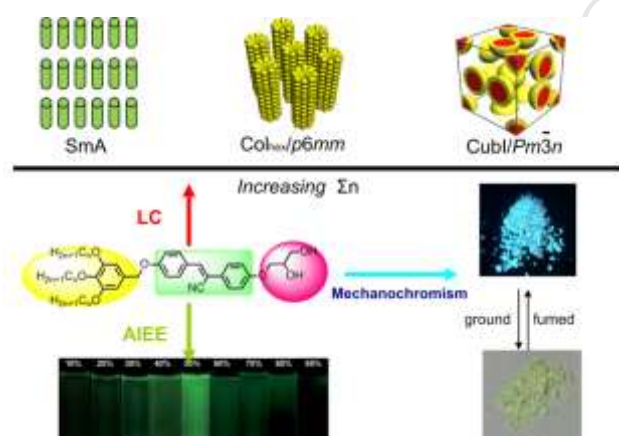
Yanming Ren,^{‡a} Ruilin Zhang,^{‡ab} Chao Yan,^a Tingyan Wang,^{ca} Huifang Cheng,^a Xiaohong Cheng^{*a}

^aKey Laboratory of Medicinal Chemistry for Natural Resources, Yunnan University, Kunming 650091, P. R. China

^bForensic Medicine of Kunming Medical University, Kunming 650500, P. R. China

^cCollege of Science, Beijing University of Chemical Technology, Beijing 100029, P.R.China

[‡]Both authors contributed equally to this work





Self-assembly, AIEE and mechanochromic properties of amphiphilic α -cyanostilbene derivatives

Yanming Ren,^{‡a} Ruilin Zhang,^{‡ab} Chao Yan,^a Tingyan Wang,^{ca} Huifang Cheng,^a Xiaohong Cheng^{*a}

^aKey Laboratory of Medicinal Chemistry for Natural Resources, Yunnan University, Kunming 650091, P. R. China

^bForensic Medicine of Kunming Medical University, Kunming 650500, P. R. China

^cCollege of Science, Beijing University of Chemical Technology, Beijing 100029, P.R.China

[‡]Both authors contributed equally to this work

ARTICLE INFO

Article history:

Received

Received in revised form

Accepted

Available online

Keywords:

α -Cyanostilbene derivatives

Liquid crystals

Aggregation-induced enhanced emission

Organogels

Mechanochromism

ABSTRACT

A series of amphiphilic α -cyanostilbene derivatives consisting of an α -cyanostilbene rodlike core with lipophilic and flexible alkyl chains at one end and a polar glycerol group at the opposite end have been synthesized and investigated by polarizing microscopy, DSC, X-ray scattering, SEM, UV-vis spectroscopy and photoluminescence measurements. These compounds can self-assemble into liquid crystalline phase sequence of SmA- Col_{hex}/p6mm- Cub_I/ Pm $\bar{3}$ n in the bulk states and multistimuli responsive organogels in organic solvents. They have reversible photoresponsive properties in solution, liquid crystalline state and gel state. They also show aggregation-induced enhanced emission (AIEE) property, meanwhile, they present excellent mechanochromic behavior and have a good reversibility of fluorescence conversion upon grinding-fuming process.

2017 Elsevier Ltd. All rights reserved.

1. Introduction

π -Conjugated α -cyanostilbene derivatives have attracted great interesting because of their tunable photophysical properties, self-assembling characteristics,^{1,2} charming functionalities, such as aggregation-induced enhanced emission (AIEE) effect,^{1,3} solid-state emission, photochromism,⁴ photovoltaics⁵ and biological imaging⁶ etc. Nanoparticles,⁷ nanowires,⁸ organogels,⁹ monolayers,¹⁰ quantum dots,¹¹ single crystals¹² and polycrystalline films¹³ based on π -conjugated α -cyanostilbene derivatives have been reported. Relevant relationship among molecular structure, self-assembly and optical property has been carefully reviewed recently.¹ The excellent characteristics of the α -cyanostilbene chromophore could be combined with the self-assembly of liquid crystals (LCs).¹⁴ Till now, few examples of α -cyanostilbene based calamitic,^{14a,15} star shaped,¹⁶ banana-shaped,¹⁷ polycatenar LCs^{4e,18} with formation of columnar,^{17,18} nematic¹⁵ or smectic phases^{17,19} have been reported. These materials have led to interesting phenomena such as fluorescence switching,¹⁹ photoisomerization-induced phase transitions^{18,19} and surface relief gratings,^{7c,14e, 20} photoisomerization-induced phase separation,²¹ and NLO^{17b} etc. However, so far as we know there are few amphiphilic α -cyanostilbene LCs been explored, and 3D spherical cubic mesophase has never been observed for α -cyanostilbene derivatives.

Herein we reported the design, synthesis, self-assembly as well as AIEE, mechanochromic properties of a series of amphiphilic α -cyanostilbenes, consisting of a α -cyanostilbene rodlike core with lipophilic flexible alkyl chains at one end and a glycerol group at opposite end. Amphiphilic LCs²² involving glycerol units are potentially useful for the design of nanostructured 1D, 2D or 3D ion conduction materials in combination with ionic liquids etc.²³

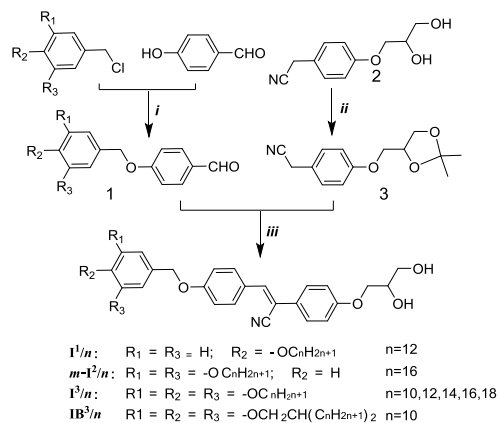
These amphiphilic α -cyanostilbenes are assigned as **I^m/n** and **IB^m/n**, where *m* stands for the number of the terminal alkyl chain, *n* is the alkyl chain length, B means that the terminal alkyl chains are the branching ones. The influence of the number, length and type of the terminal alkyl chains on the self-assembly of these compounds was investigated. These compounds can self-assemble into LCs and gels. They have photoresponsive ability in solution, LC state and gel state, additionally they show the AIEE and excellent mechanochromic behaviors. Therefore these compounds could be considered as multifunctional materials.

2. Results and discussion

2.1. Synthesis

The target compounds **I^m/n** and **IB^m/n** have been synthesized via Knoevenagel reactions between benzaldehydes **1** with phenylacetonitrile **3** as shown in Scheme 1. Firstly 4-hydroxybenzaldehyde was etherified with appropriate

alkylsubstituted benzyl chlorides, leading to phenyl aldehydes **1**. **3** was prepared from 2-(4-hydroxyphenyl)acetonitrile by etherification with glycidol,²⁴ followed by protection of the 1,2-diol group as 1,2-isopropylidene ketal.²⁵ Knoevenagel reactions between benzaldehydes **1** with phenylacetonitrile **3**, followed by deprotection of the 1,2-O-isopropylidene glycerol units yielded the final compounds.



Scheme 1. Synthesis of compounds I^m/n and IB^m/n ; *Reagents and conditions:* i) DMF, K_2CO_3 , reflux, 80 °C, 10 h, 54-89%; ii) PPTS, 2,2-dimethoxypropane, THF, 40 °C, 3 h; iii) 4-hydroxybenzyl cyanide, tert-butanol, potassium tert-butoxide, 70 °C, reflux, 12 h, 33-43%.

2.2. Mesomorphic properties

The LC properties of compounds I^m/n and IB^m/n were studied by polarizing optical microscopy (POM, Optiphot 2, Nikon, in

Table 1. Transition temperatures and associated enthalpy values (in brackets) of compounds $I^1/12$, *meta*- $I^2/16$, I^3/n and $IB^3/10$ ^a

Comp	R_1, R_2, R_3	$T/^\circ C$ [$\Delta H/kJ mol^{-1}$]
$I^1/12$	$R_1 = R_3 = H, R_2 = -OC_{12}H_{25}$	Cr 69.4 [17.8] SmA 121.2 [2.7] Iso
<i>meta</i> - $I^2/16$	$R_1 = R_3 = -OC_{12}H_{25}, R_2 = H$	Cr 70.9 [27.8] Col _h 116.2 [0.2] Iso
$I^3/10$	$R_1 = R_2 = R_3 = -OC_{10}H_{21}$	Cr < 20 Col _h 153 [0.2] Iso
$I^3/12$	$R_1 = R_2 = R_3 = -OC_{12}H_{23}$	Cr 28 [30.2] Col _h 143 [0.2] Iso
$I^3/14$	$R_1 = R_2 = R_3 = -OC_{14}H_{29}$	Cr 43 [21.5] Col _h 125 [0.1] Iso
$I^3/16$	$R_1 = R_2 = R_3 = -OC_{16}H_{33}$	Cr 66.4 [26.9] Col _h 98.1 [0.04] Iso
$I^3/18$	$R_1 = R_2 = R_3 = -OC_{18}H_{37}$	Cr 60 [42.7] Col _h 88 [0.2] Iso
$IB^3/10$	$R_1 = R_2 = R_3 = -OCH_2CH(C_{10}H_{21})_2$	Cr 63.5 [11.0] Cub _I / $Pm\bar{3}n$ 85 ^b Iso

^aTransition temperatures were determined by DSC (peak temperature from heating scans, at a rate of 1 K min⁻¹ for $I^2/16$, I^3/n ; 2 K min⁻¹ for compounds $I^1/12$, and 5 K min⁻¹ for $IB^3/10$, melting transitions were measured in the first heating scan), abbreviations: Cr = crystal; SmA = smectic A phase; Col_h = hexagonal columnar phase; Cub_I/ $Pm\bar{3}n$ = micellar cubic mesophase with space groups $Pm\bar{3}n$; Iso = isotropic liquid. ^bTransition temperature was determined by POM.

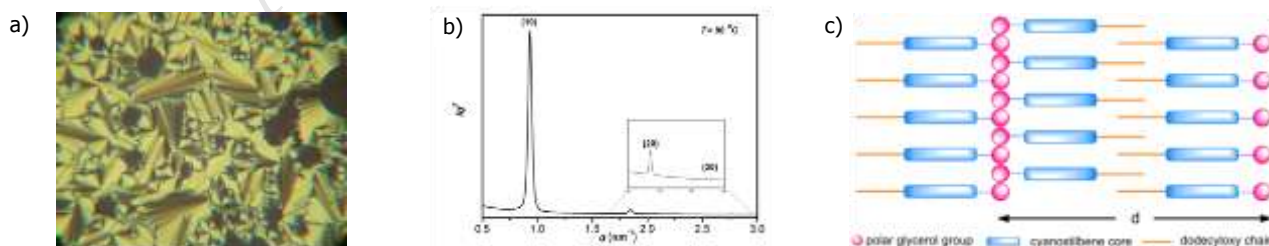


Fig. 1 (a) Texture of SmA phase as seen between crossed polarizers at $T = 95$ °C on cooling process; (b) SAXS diffractogram of the SmA phase at $T = 90$ °C; (c) model of SmA₂ phase of compound $I^1/12$.

conjunction with a FP 82 HT heating stage, Mettler), differential scanning calorimetry (DSC, NETZSH 200F3) and X-ray diffraction (XRD) techniques. The transition temperatures of the synthesized α -cyanostilbenes I^m/n and $IB^3/10$ are reported in Table 1.

2.2.1. Compounds ($I^1/12$, *meta*- $I^2/16$, I^3/n) and their formation of smectic and columnar phases

Smectic A phase was observed in single chain compound $I^1/12$ and columnar phases were observed in two alkyl chain compound *meta*- $I^2/16$ and triple alkyl chain compounds I^m/n ($m = 3, n = 10, 12, 14, 16, 18$). Compound $IB^3/10$ with triple branching alkyl chains shows a cubic phase. The smectic A phase of single chain compound $I^1/12$ was characterized by its typical fan-shaped focal conics textures²⁶ (Fig. 1a). The small-angle X-ray scattering (SAXS) pattern of $I^1/12$ shows three equidistant peaks ($d_{10} = 6.731$ nm, $d_{20} = 3.407$ nm, $d_{30} = 2.281$ nm) with reciprocal d -spacing ratio of 1 : 2 : 3, which confirms a layer structure. The layer spacing in the SmA phase of compound $I^1/12$ is $d = 6.731$ nm (Table. S1). Compared with the molecular length in the most stretched conformation ($L = 3.69$ nm, see Table 2), the layer thickness is larger than twice the molecular length ($d/L = 1.82$), but slightly smaller than twice the length, indicating a bilayer structure with slightly intercalation of the alkyl chains (SmA₂). In this SmA₂ structure there is a non-intercalated antiparallel end-to-end packing of the aromatic cores, allowing the segregation of the polar glycerol units from the less polar alkyl-substituted benzene rings at the opposite end, and the reduction of the d value is in this case due to the intercalation of the alkyl chains (Fig. 1c).

Two chain compound *meta-I*²/16 and triple chain compounds *I*³/*n* (*n* = 10, 12, 14, 16, 18) exhibit enantiotropic columnar phases. Increasing chain number and length leads to a dramatic reduction of the stability of the columnar phases as seen by comparison of compounds *I*³/*n* (*n* = 10, 12, 14, 16, 18), in which the Col-to-Iso transition is reduced by more than 105 K (Table 1). The columnar phases were identified by the typical spherulitic fanlike textures under POM (Fig. 2a and Fig. S1a-e). Investigation of the columnar phases by POM with an additional λ -retarder plate (Fig. 2a and Fig. S1a-e) indicates that the columnar phases of compounds *meta-I*²/16, *I*³/*n* (*n* = 10, 12, 14, 16, 18) are optically negative.²⁷ This means that the major intramolecular π -conjugation pathway, which is along the long axis of the aromatic cores, is perpendicular to the column long axis. The columnar phases were also investigated by small-angle X-ray scattering (SAXS) (Fig. 2b and Fig. S3). The X-ray diffraction pattern of compound *I*³/12 is shown as an example in Fig. 2b. There are three small angle reflections with a ratio of their reciprocal spacing 1 : 3^{1/2} : 2, which can be indexed to the 10, 11, 20 reflections of hexagonal lattice with *p6mm* symmetry. The lattice parameters *a* were calculated to be 5.6~5.9 nm for the columnar phases of these compounds (Table 2 and Tables S2-S7). The number of molecules organized in a slice of the columns with a height of *h* = 0.45 nm (a typical value for the maximum of the diffuse wide angle scattering) *u*, estimated using equation (1) and assuming a density of $\rho = 1 \text{ g/cm}^3$ is between *u* = 7 to 9 for the investigated compounds (N_A = Avogadro constant; *M* = molecular mass, see Table 2).

$$u = \left(\frac{a^2}{2}\right) \sqrt{3}h (N_A/M)\rho \quad (1)$$

There is a slight decrease of this number with increasing chain number and length, which is due to the increase of the taper angle with the increasing space requirement of the terminal alkyl chains.^{28,29} The three alkyl chains of *I*³/18 provide a stronger interface curvature, leading to a clear decrease of the number of molecules (*u* = 6.9) organized in the cross section of the column, as compared to the number *u* = 9.2, 7.7, 7.5, 7.3 and 7.9 for *I*³/*n* (*n* = 10, 12, 14, 16) and *meta-I*²/16 respectively. The number of molecules *u* = 7.9 of compound *meta-I*²/16 is nearly the same as *u* = 7.7-7.3 for the compounds *I*³/*n* (*n* = 12, 14, 16) with triple medium length of alkyl chains. Therefore it can be assumed that the taper angle of the *meta* substituted double chain compound *meta-I*²/16 were almost the same as those of triple chain compounds *I*³/*n* (*n* = 12, 14, 16).

The introduction of the second or the triple alkyl chains induces a change of the molecular shape from rodlike (compounds *I*³/12) to taper shape, leading to an organization of the molecules in circular cylindrical aggregates, which can organize into a hexagonal lattice. This is very similar to observations made with other taper amphiphiles.³⁰ Therefore 7-9 molecules self-assemble into an overall disk-like stratum and they successively stack one another to form supramolecular columns (Fig. 2d and Fig. S5). The polar units form the column centers, which are surrounded by the rigid α -cyanostilbene aromatic cores, and assembled on a hexagonal lattice within the lipophilic continuum mainly formed by the terminal alkyl chains. The effective diameters of the columns correspond to the experimentally observed hexagonal lattice parameters *a*_{hex}. These models are also supported by the electron density maps (Fig. S4), which were reconstructed from the small-angle X-ray scattering (SAXS) intensities of compounds *meta-I*²/16 (Fig. S3a), *I*³/10 (Fig. S3b), *I*³/12 (Fig. 2b), *I*³/14 (Fig. S3c), *I*³/16 (Fig. S3d) and *I*³/18 (Fig. S3e), where the column centers with high electron density (purple) are surrounded by medium electron density shells (blue/green/yellow).

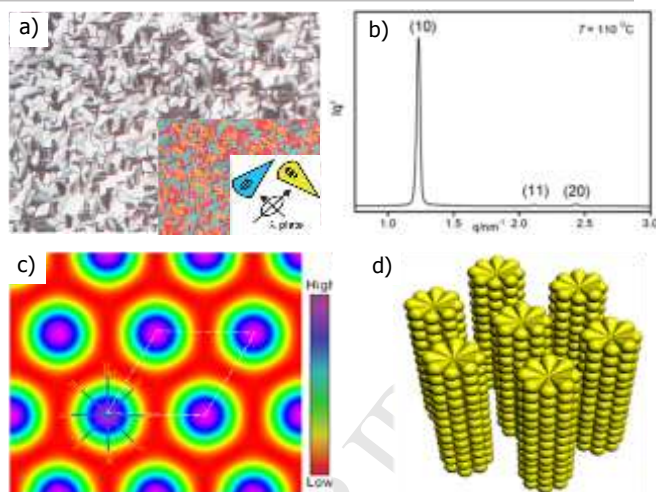


Fig. 2 Characterization of compound *I*³/12: (a) Texture as seen between crossed polarizers at *T* = 118 °C (inset shows the same region with λ -plate); (b) SAXS diffractogram of the Col_{hex} phase of *I*³/12 at *T* = 110 °C; (c) Reconstructed electron density map for the Col_{hex} phase of *I*³/12; (d) Model for molecular packing of compound *I*³/12 in Col_{hex} phase.

Table 2. Comparison of X-ray data and molecular dimensions of the columnar and cubic phases of compounds *I*^{*m*}/*n* and *IB*³/10^a

Comp.	Phase, Plane/space group	<i>L</i> [nm]	<i>a</i> [nm] (<i>T</i> [°C])	<i>u</i>
<i>I</i> ¹ /12	SmA	3.69	/	/
<i>m-I</i> ² /16	Col _{hex} / <i>p6mm</i>	4.23	5.7 (100)	7.9
<i>I</i> ³ /10	Col _{hex} / <i>p6mm</i>	3.51	5.8 (90)	9.2
<i>I</i> ³ /12	Col _{hex} / <i>p6mm</i>	3.69	5.6 (110)	7.7
<i>I</i> ³ /14	Col _{hex} / <i>p6mm</i>	3.93	5.8 (115)	7.5
<i>I</i> ³ /16	Col _{hex} / <i>p6mm</i>	4.22	5.8 (90)	7.3
<i>I</i> ³ /18	Col _{hex} / <i>p6mm</i>	4.47	5.9 (80)	6.9
<i>IB</i> ³ /10	Cub/ <i>Pm</i> $\bar{3}$ <i>n</i>	3.67	11.18 (75)	72.8

^aAbbreviations: *a* = lattice parameter determined by XRD (*a*_{hex} and *a*_{cub}, respectively); *L* = maximum molecular length in the most extended conformation; *u* = number of molecules in the cross section of a column in the Col_{hex} phases (with assumed height of 0.45 nm) or number of molecules in each aggregate of the Cub/*Pm* $\bar{3}$ *n* lattice (*u*_{cell}/8).

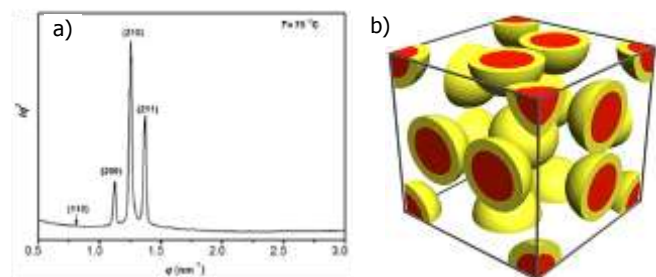


Fig. 3 (a) SAXS diffractograms of compound *IB*³/10; (b) Possible model for molecular organization micellar cubic phase.

2.2.2. Compound *IB*³/10 and formation of micellar cubic phases

Interestingly, micellar *Pm* $\bar{3}$ *n* cubic phase was observed in compound *IB*³/10 with triple branching alkyl chains. For this cubic phase, under POM, optically isotropic texture was observed, which is not fluid, but soft and viscoelastic, by increasing the temperature, sharp transitions to highly fluid isotropic liquids occur at defined temperature (Fig. S1f). In the

cubic phase of compound **I³/10**, the positions of the sharp powderlike reflections in the small-angle region can be indexed to be a cubic phase with space group of $Pm\bar{3}n$ with lattice parameter $a_{\text{cub}} = 11.18 \text{ nm}$ (Fig. 3a and Table 2 and Table S8). The $Pm\bar{3}n$ lattice is the most commonly observed lattice of micellar cubic phases (Cub_I) (Fig. 3b), occurring in thermotropic systems formed by spheroidal aggregates with soft corona.³¹ In this type of cubic phase, the molecules are organized in closed spheroidal aggregates, and there are eight of these aggregates in each unit cell. By calculation, each micelle is built up of approximately 73 molecules in the $Pm\bar{3}n$ cubic phase of **I³/10**. The spheroids should have a core shell structure with a hydrophilic cores formed by the polar glycerol groups which were surrounded by π -conjugated stratum, these core-shell spheroids are encapsulated by the terminal alkyl chain moieties in the micelles (Fig. 3b). The large volume of the flexible chains gives rise to a large interface curvature, thus contributes to the emergence of the cubic phase. The twist-bend α -cyanostilbene core and possible *trans-cis* transformation of central unit could lead to the relatively flexible rigid core, contribute to the formation of softness of these spheres in cubic phase, and this is favorable for the organization in a $Pm\bar{3}n$ lattice instead of other cubic phases.

Therefore the structure-property relationship of the amphiphilic α -cyanostilbene derivatives focusing on the impact of the number, length and type of terminal alkyl chains on the self-assembly into lamellar, columnar, and spheroidal supermolecular aggregates are systematically studied. By increasing the volume ratio of the terminal alkyl chains, namely increasing the number and length of the alkyl chains or branching the alkyl chains, the interface curvature between the nanosegregated regions of the α -cyanostilbene cores and the flexible chains should be increased, the molecular shapes have been changed from rodlike to taper shapes. This structural variation gives rise to the transition from the bilayer smectic phases through hexagonal columnar (Col_{hex}) to cubic ($\text{Cub}_I/Pm\bar{3}n$) LC phases. So far as we know, the Cub_I phase as well as the bilayer smectic phase are firstly realized here for the α -cyanostilbene derivatives.

2.3. Photoisomerization behavior in liquid crystalline and solution

The effect of *trans-to-cis* photoisomerization caused by the UV irradiation on the thermotropic LC phases of these compounds was investigated. All the liquid crystalline phases can respond to the UV irradiation immediately by change their textures to isotropic states and recover to their original textures after removing the UV source. This means that all the compounds showed *trans* to *cis* photoisomerization under UV irradiation and *cis* to *trans* isomerization under visible light irradiation. For example, sample **I³/12** was cooled from the isotropic liquid state to 115 °C in the range of the Col_{hex} phase (Fig. 4a). After annealing for 5 minutes the sample was exposed to UV irradiation at 365 nm (10 mW cm^{-2}) for 3s, the birefringence texture of the Col_{hex} phase was disappeared and replaced by isotropic one (Fig. 4a-b). After removal of the UV lamp, the birefringence texture of the Col_{hex} phase was recovered (Fig. 4b-a). It seems that the *trans-to-cis* photoisomerization effect on the liquid crystalline property of the compound reported here is very strong. Similarly, the homologous series compounds showed photoisomerization reversible transition of Col_{hex} -Iso. Additionally the homologous compounds also showed photoisomerization reversible transition in solution (Fig. S6).

Such photoisomerizations could be useful for light sensitive displays or for data storage applications.^{32,33}

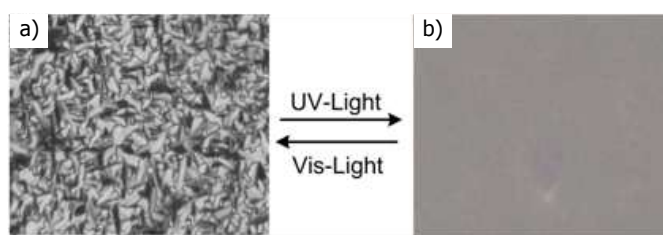


Fig. 4 Textural changes as observed by POM at the photo induced Col_{hex} -Iso transitions and the relaxation Iso- Col_{hex} as observed for compound **I³/12** at 115 °C: (a) before UV irradiation; (b) after UV irradiation.

2.4. Gelation properties

The gelation ability of these compounds was evaluated by using compound **I³/12** as a representative in various organic solvents at a concentration of 5.0 mg/mL, and the results are summarized in Table 3. **I³/12** can gelate in ethanol and methanol, solve in CHCl_3 , toluene and THF. Whereas it is insoluble in *n*-butanol and acetone, and precipitates in cyclohexane and DMSO. So far as we know there is few gelation behavior of α -cyanostilbene derivatives been reported.⁹ Intermolecular hydrogen bonds, π - π interactions and intramolecular hydrogen bonds as well as van der Waals forces should play an important role for the aggregation of the compound in solvents.³⁴ Under irradiation of UV lamp, the non luminescence gel become blue luminescence (Fig. 5). The organogels exhibit multiple stimuli-responsive behaviors namely gel-sol reversible process upon exposure to a number of environmental stimuli including light, temperature and shear etc (Fig. 6b). Irradiation with UV light, application of heat or shear resulted in a sol state through disruption of the non-covalent interactions between the molecules. The gel state can be recovered by removal of such stimuli. Such multiple stimuli-responsive behaviors could be useful for drug controlled release,³⁵ energy transfer,³⁶ hardeners of solvents and sensors etc.³⁷ In order to obtain a visual insight into the morphologies of the molecular aggregation model, the gel was investigated by scanning electron microscopy (SEM). The SEM image of the xerogel formed by **I³/12** (Fig. 6a) shows the formation of three-dimensional networks composed of entangled fibrous aggregates. The approximate diameter of the fibers is 80-130 nm.



Fig. 5 Photograph of solution and gels prepared with **I³/12** in ethanol, 10^{-6} M , $T = 20 \text{ }^\circ\text{C}$. (a) without irradiation; (b) under irradiation with 365 nm light.

DMF	335 nm	465 nm	464 nm	130 nm
Acetonitrile	338 nm	473 nm	470 nm	135 nm

^a λ_{ex} = maxima absorption wavelength; ^b $\lambda_{\text{ex}} = 330$ nm; ^cThe Stokes shift was obtained from the difference of the emission and absorption maximum ($\Delta\lambda_{\text{ST}} = \lambda_{\text{em}}^{\text{a}} - \lambda_{\text{abs}}$).

wavelengths of compound **I³/12** exhibited red-shifts of 11 nm, and the emission maximum of **I³/12** exhibited bathochromic shifts of 40 nm from hexane to acetonitrile, respectively. Meanwhile, Stokes shifts are also increased dramatically from hexane to acetonitrile. To have a better insight into the ICT process, the density functional of B3LYP with 6-31G* basis sets was used to investigate the electron cloud distribution (Fig. 7c). The electron cloud of the highest occupied molecular orbital (HOMO) was mainly localized on the linear π -conjugated systems, while the electron cloud of the lowest unoccupied molecular orbital (LUMO) was localized on the α -cyanostyrene unit due to the strong electron withdrawing ability of the cyano group. Compound **I³/12** exhibited obviously charge separation and indicated a typical intramolecular charge transfer (ICT) effect.

2.6. Aggregation-induced emission enhancement performances

Compound **I³/12** is soluble in common organic solvents in low concentration, such as CH_2Cl_2 , THF, ethyl acetate and almost insoluble in water. To investigate the AIEE characteristic of **I³/12**, its UV-vis and fluorescence spectra with different fraction of water were studied (Fig. 8). The concentration of this compound was kept at 1×10^{-5} mol L^{-1} . For UV-vis spectra of compound **I³/12** (Fig. 8a), with an increasing fraction of water from 0 to 30%, the absorption band almost remained at the same position of 325 nm. With up to 40% of water content, molecules began to form aggregates, and the absorption band showed red-shifts slightly. The possible reasons are that the increase of the polarity and the planarization of a twisted molecule caused the extension of the effective conjugation lengths in the aggregated state.³⁹

For the fluorescence intensity, compound **I³/12** showed a dramatic change from weakly emitting in the monomolecular state to strongly fluorescent in the aggregated state (Fig. 8b). When the water fraction is inferior to 30%, the fluorescence intensity of compound **I³/12** emitted weakly fluorescence emission, whereas in the case of 40% volume fractions of water addition, the molecule began aggregating and the fluorescence intensity promptly increased and reached the maximum value at 50%. Meanwhile, the aggregates exhibit an enhancement of green-yellow emission under UV irradiation.

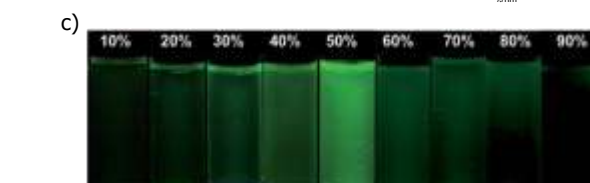
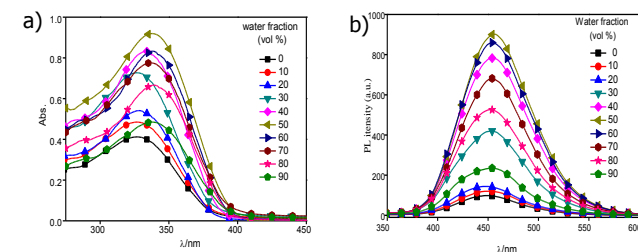


Table 3. Gelation properties of **I³/12**^a

Solvent	I³/12	Solvent	I³/12
CHCl_3	S	CH_2Cl_2	S
Ethyl acetate	S	Cyclohexane	P
Hexane	S	Ethanol	G
Methanol	G	<i>n</i> -Butanol	I
Acetone	I	Toluene	S
DMSO	P	THF	S

^aS = solution, P = precipitation, G = gelation, I = insoluble, gels formed at room temperature (20 °C).

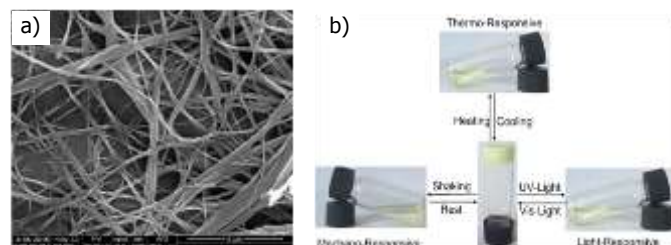


Fig. 6 (a) SEM images of xerogel formed by compound **I³/12** in ethanol, scale bar is 5 μm ; (b) compound **I³/12** in ethanol (5.0 mg/ml), photograph of multistimuli responsive organogels.

2.5. Solvent effect

The UV-vis and fluorescence spectra of compound **I³/12** in different solvents (hexane, toluene, dichloromethane (DCM), tetrahydrofuran (THF), acetonitrile, N,N-dimethylformamide (DMF)) are shown in Fig. 7 and Fig S7, the corresponding photophysical data are summarized in Table 4. As we know, the solvents can change the energy levels of the absorption or emission bands. As depicted in Fig. 7a, compound **I³/12** shows one characteristic absorption band at about 330 nm in varying solvents, which is attributed to the π - π^* and intramolecular charge transfer (ICT) transitions.³⁸ It can be obviously observed that the absorption

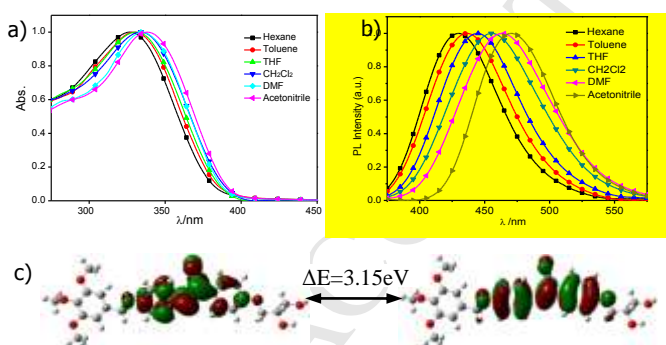


Fig. 7 The UV-vis spectra (a) and fluorescence spectra ($\lambda_{\text{ex}} = 330$ nm) (b) of compound **I³/12** in different solvents (1×10^{-5} mol L^{-1}); (c) molecular orbital amplitude plots of the HOMO and LUMO levels, energy gaps and electron cloud distribution of **I³/12** calculated using the B3LYP/6-31G* basis set.

Table 4. UV-vis absorption and fluorescence spectroscopy data of compound **I³/12**

Compd.	Solvent	λ_{abs}	$\lambda_{\text{em}}^{\text{a}}$	$\lambda_{\text{em}}^{\text{b}}$	$\Delta\lambda_{\text{ST}}^{\text{c}}$
I³/12	Hexane	327 nm	431 nm	430 nm	104 nm
	Toluene	330 nm	437 nm	436 nm	107 nm
	THF	331 nm	445 nm	444 nm	114 nm
	DCM	334 nm	459 nm	456 nm	125 nm

Fig. 8 The UV-vis absorption (a) and fluorescence spectra (excited at 326 nm, 327 nm, 328 nm, 328 nm, 333 nm, 338 nm, 337 nm, 337 nm, 338 nm, 338 nm respectively) (b) of compound **I³/12** in ethanol–water mixtures with different water volume fractions; (c) optical photographs recorded under 365 nm UV irradiation with various fractions of water.

The mechanism of AIEE may be attributed to the restriction of intramolecular rotation (RIR) and intermolecular interaction.⁴⁰ When the fraction of water is higher than 60%, the fluorescence intensity gradually decreases. This phenomenon is reasonable that aggregates begin to form and precipitate quickly at high water content. This process leads to the decrease of fluorescent species and lowers the fluorescence intensity. The other compounds **I³/n** have been found to display a similar behavior.

2.7. Mechanofluorochromic properties

The AIEE feature may be suggested that those compounds could be used as stimuli responsive smart materials. To check whether compound **I³/12** has the mechanofluorochromic property, its emission property was studied in the solid state. It emitted green light after grinding with a spatula for 3 min. As shown in Fig. 9, the emission peak showed an obvious red shift for **I³/12** from 437 nm to 455 nm. When fuming with ethanol vapor for 5 min, the emission peak almost returned to the original fluorescence emission. For the UV-vis spectra of **I³/12** in different states (Fig. S8), it was found that the maximum absorption peaks of the solid state showed an obvious red-shift compared with that in dilute solution, mainly due to the reason that effective conjugation increased through intermolecular interaction in the solid state. Meanwhile, the absorption peak appeared to red-shift after grinding (from 345 nm to 358 nm, Fig. S9), which suggested that the molecular conformation became more planarized and further increased the conjugation degree. The results indicated that the pressure of grinding changes not only the absorption spectra but also the emission spectra. The conversion between the green and blue emission can be repeated many times without fatigue due to the nondestructive nature of the stimuli.^{20b}

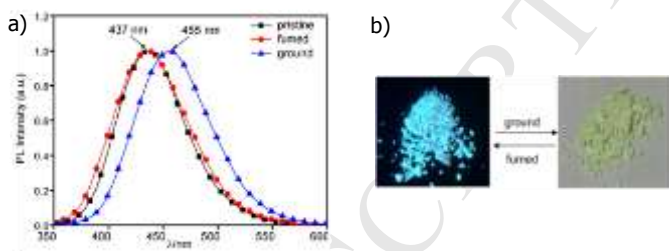


Fig. 9 (a) Emission spectra of pristine, ground and fumed with ethanol samples of compound **I³/12**. ($\lambda_{\text{exc}} = 345 \text{ nm}$) (b) Photographs of pristine and ground powders under 365 nm light.

3. Conclusion

In summary, novel amphiphilic α -cyanostilbene derivatives **I^m/n** and **IB^m/10** have been synthesized. All of these compounds exhibit enantiotropic liquid crystalline phases, increasing the volumetric ratio of the terminal alkyl chains, not only bilayer smectic A and columnar phases, but also $Pm\bar{3}n$ micellar cubic phase are found in these compounds. The formation of the micellar cubic phase is due to the larger interface curvature between the flexible chains and the polar regions. The reversible photoresponsive behavior of these compounds in liquid crystals,

solutions and gels states was well demonstrated. In addition, compounds **I^m/n** exhibited AIEE properties attributed to the restriction of intramolecular rotation (RIR) and intermolecular interaction. Meanwhile, the emission peak of compound **I^m/n** was obviously red-shifted after grinding. Such multifunctional materials should have great potentials in displays, photochemical molecular switches, AIEE materials and mechano fluorochromic materials etc.

Acknowledgements

This work was supported by the National Natural Science Foundation of China [no. 21664015, 21364017] and Yunnan Provincial Department of Education Foundation [no. ZD2015001], the Yunnan University Graduate Research Foundation Project [no. YNUY201682, YNUY201620]. The calculations were performed with the support of the Yunnan University Supercomputer Center. We thank beamline 1W2A at Beijing Accelerator Laboratory and beamline BL16B1 at Shanghai Synchrotron Radiation Facility (SSRF), China.

References

1. An B-K, Gierschner J, Park SY. *Acc. Chem. Res.* 2012; 45: 544-554.
2. Zhu LL, Zhao YL. *J. Mater. Chem. C.* 2013; 1: 1059-1065.
3. (a) An B-K, Kwon S-K, Jung, S. D, Park SY. *J. Am. Chem. Soc.* 2002; 124: 14410-14415; (b) Gierschner J, Park SY. *J. Mater. Chem. C.* 2013; 1: 5818-5832.
4. (a) Chung JW, You YG, Huh HS, An B-K, Yoon S-J, Kim SH, Lee SW, Park SY. *J. Am. Chem. Soc.* 2009; 131: 8163-8172; (b) Yoon SJ, Chung JW, Gierschner J, Kim KS, Choi M-G, Kim D, Park SY. *J. Am. Chem. Soc.* 2010; 132: 13675-13683; (c) Chung JW, Yoon S-J, An B-K, Park SY. *J. Phys. Chem. C.* 2013; 117: 11285-11291; (d) Kwon MS, Gierschner J, Seo J, Park SY. *J. Mater. Chem. C.* 2014; 2: 2552-2557; (e) Park JW, Nagano S, Yoon S-J, Dohi T, Seo J, Seki T, Park SY. *Adv. Mater.* 2014; 26: 1354-1359.
5. (a) Mikroyannidis JA, Kabanakis AN, Sharma SS, Sharma GD. *Adv. Funct. Mater.* 2011; 21: 746-755; (b) Li XJ, Xu YX, Li F, Ma YG. *Org. Electron.* 2012; 13: 762-766; (c) Jia WB, Yang P, Li JJ, Yin ZM, Kong L, Lu HB, Ge ZS, Wu YZ, Hao XP, Yang JX. *Polym. Chem.* 2014; 5: 2282-2292.
6. (a) Lim C-K, Kim S, Kwon IC, Ahn C-H, Park SY. *Chem. Mater.* 2009; 21: 5819-5825; (b) Zhang XQ, Zhang, XY, Yang B, Yang Y, Wei Y. *Polym. Chem.* 2014; 5: 5885-5889.
7. (a) Lim S-J, An B-K, Jung SD, Chung M-A, Park SY. *Angew. Chem., Int. Ed.* 2004; 43: 6346-6350; (b) Nam H, Boury B, Park SY. *Chem. Mater.* 2006; 18: 5716-5721; (c) Zhang Y, Sun J, Bian G, Chen YY, Ouyang M, Hu B, Zhang C. *Photochem. Photobiol. Sci.* 2012; 11:1414-1421.
8. (a) An B-K, Gihm SH, Chung JW, Park CR, Kwon S-K, Park SY. *J. Am. Chem. Soc.* 2009; 131: 3950-3957; (b) Kim JH, Watanabe A, Chung JW, Jung Y, An B-K, Tada H, Park SY. *J. Mater. Chem.* 2010; 20: 1062-1064; (c) Yun SW, Kim JH, Shin S, Yang H, An B-K, Yang L, Park SY. *Adv. Mater.* 2012; 24: 911-915; (d) Shin S, Gihm SH, Park CR, Kim S, Park SY. *Chem. Mater.* 2013; 25: 3288-3295; (e) Jin YZ, Xia YJ, Wang S, Yan L, Zhou Y, Fan J, Song B. *Soft Matter.* 2015; 11: 798-805.
9. (a) An B-K, Lee D-S, Lee J-S, Park Y-S, Song H-S, Park SY. *J. Am. Chem. Soc.* 2004; 126: 10232-10233; (b) Chung JW, An B-K, Park SY. *Chem. Mater.* 2008; 20: 6750-6755; (c) Yoon S-J, Kim JH, Chung JW, Park SY. *J. Mater. Chem.* 2011; 21: 18971-18973; (d) Seo J, Chung JW, Cho I, Park SY. *Soft Matter.* 2012; 8: 7617-7622; (e) Seo J, Chung JW, Kwon JE, Park SY. *Chem. Sci.* 2014; 5: 4845-4850.
10. Gulino A, Lupo F, Condorelli GG, Fragala ME, Amato ME, Scarlata G. *J. Mater. Chem.* 2008; 18: 5011-5018.
11. Zhu LL, Ang CY, Li X, Nguyen KT, Tan SY, Ågren H, Zhao YL. *Adv.*

- Mater.* 2012; 24: 4020-4024.
12. (a) Li Y, Shen FZ, Wang H, He F, Xie ZQ, Zhang HY, Wang ZM, Liu LL, Li F, Hanif M, Ye L, Ma YG. *Chem. Mater.* 2008; 20: 7312-7318;
(b) Varghese S, Yoon S-J, Calzado EM, Casado S, Boj PG, Díaz-García MA, Resel R, Fischer R, Milián-Medina B, Wannemacher R, Park SY, Gierschner J. *Adv. Mater.* 2012; 24: 6473-6478;
(c) Park SK, Varghese S, Kim JH, Yoon S-J, Kwon OK, An B-K, Gierschner J, Park SY. *J. Am. Chem. Soc.* 2013; 135: 4757-4764.
 13. Kunzelman J, Kinami M, Crenshaw BR, Protasiewicz JD, Weder C. *Adv. Mater.* 2008; 20:119-122.
 14. (a) Percec V, De Souza Gomes A, Lee M. *J. Polym. Sci.* 1991; 29: 1615-1622;
(b) Tsibouklis J, Richardson PH, Ahmed AM, Richards RW, Feast WJ. *Synth. Met.* 1993; 61: 159-162;
(c) Aoki H, Mihara T, Koide N. *Mol. Cryst. Liq. Cryst.* 2004; 408: 53-70;
(d) Bao R, Pan M, Zhou Y, Qiu JJ, Tang HQ, Liu CM. *Synth. Commun.* 2012; 42: 1661-1668;
(e) Mao WG, Chen K, Ouyang M, Sun JW, Zhou YB, Song QB, Zhang C. *Acta Chim. Sin.* 2013; 71: 613-618.
 15. (a) Wei RB, He YN, Wang XG, Keller P. *Macromol. Rapid Commun.* 2014; 35: 1571-1577;
(b) Morris SM, Qasim MM, Gardiner DJ, Hands PJW, Castles F, Tu G, Huck WTS, Friend RH, Coles HJ. *Opt. Mater.* 2013; 35: 837-842.
 16. Bao R, Pan M, Qiu JJ, Liu CM. *Chin. Chem. Lett.* 2010; 21: 682-685.
 17. (a) Martínez-Abadía M, Varghese S, Milián-Medina B, Gierschner J, Giménez R, Blanca Ros M. *Phys. Chem. Chem. Phys.* 2015; 17: 11715-11724;
(b) Martínez-Abadía M, Robls-Hernández B, Villacampa B, Giménez R, Ros MB. *J. Mater. Chem. C.* 2015; 3: 3038-3048.
 18. Yoon S-J, Kim JH, Kim KS, Chung JW, Heinrich B, Mathevet F, Kim P, Donnio B, Attias A-J, Kim D, Park SY. *Adv. Funct. Mater.* 2012; 22: 61-69.
 19. Lu HB, Zhang SN, Ding AX, Yuan M, Zhang GY, Xu W, Zhang GB, Wang XH, Qiu LZ, Yang JX. *New J. Chem.* 2014; 38: 3429-3433.
 20. (a) Zhang YJ, Sun JW, Lv XJ, Ouyang M, Fan GB, Wang W, Zhang C. *CrytEngComm.* 2013; 15: 8998-9002;
(b) Zhang YY, Li HF, Zhang GB, Xu XY, Kong L, Tan YP, Yang, JX. *J. Mater. Chem. C.* 2016; 4: 2971-2978.
 21. Lu HB, Qiu LZ, Zhang GY, Ding AX, Xu WB, Zhang GB, Wang XH, Kong L, Tian YP, Yang JX. *J. Mater. Chem. C.* 2014; 2: 1386-1389.
 22. (a) Tschierske C. *J. Mater. Chem.* 1998; 8(7): 1485-1508;
(b) Tschierske C. *Angew. Chem. Int. Ed.* 2013; 52(34): 1-53.
 23. Kato T. *Angew. Chem., Int. Ed.* 2010; 49: 7847-7848.
 24. VanRheenen V, Cha DY, Hartley WM. *Org. Synth.* 1978; 58, 43-51.
 25. Tan XP, Kong LY, Dai H, Cheng XH, Liu F, Tschierske C. *Chem. Eur. J.* 2013; 19: 16303-16313.
 26. Dierking, I. *Textures of Liquid Crystals*, Wiley-VCH, Weinheim, 2003.
 27. Cheng XH, Dng X, Wei GH, Prehm M, Tschierske C. *Angew. Chem., Int. Ed.* 2009; 48: 8014-8017.
 28. (a) Borisch K, Diele S, Goring P, Kresse H, Tschierske C. *J. Mater. Chem.* 1998; 8: 529-543;
(b) Borisch K, Diele S, Goring P, Muller H, Tschierske C. *Liq. Cryst.* 1997; 22: 427-443;
(c) Borisch K, Diele S, Goring P, Kresse H, Tschierske C. *Angew. Chem.* 1997; 109: 2188-2190;
(d) Borisch K, Tschierske C, Goring P, Diele S. *Chem. Commun.* 1998, 2711-2712.
 29. (a) Hudson SD, Jung H-T, Percec V, Cho W-D, Johansson G, Ungar G, Balagurusamy VSK. *Science.* 1997; 278: 449-452;
(b) Percec, V.; Cho W-D, Mosier PE, Ungar G, Yeardley DJP. *J. Am. Chem. Soc.* 1998; 120: 11061-11070;
(c) Percec V, Holerca MN, Uchida S, Cho W-D, Ungar G, Lee YS, Yeardley DJP. *Chem. Eur. J.* 2002; 8: 1106-1117;
(d) Yeardley DJP, Ungar G, Percec V, Holerca MN, Johansson G. *J. Am. Chem. Soc.* 2000; 122: 1684-1689;
(e) Rosen BM, Wilson CJ, Wilson DA, Peterca M, Imam MR, Percec V. *Chem. Rev.* 2009; 109: 6275-6540.
 30. Borisch K, Diele S, Goring P, Tschierske C. *Chem. Commun.* 1996, 237-238.
 31. (a) Ziherl P, Kamien RD. *J. Phys. Chem. B.* 2001; 105: 10147-10158;
(b) Grason GM, DiDonna BA, Kamien RD. *Phys. Rev. Lett.* 2003; 91: 058304.
 32. Tan XP, Li Z, Xia M, Cheng XH. *RSC Adv.* 2016; 6: 20021-20026.
 33. Westphal E, Bechtold IH, Gallardo H. *Macromolecules* 2010; 43: 1319-1328.
 34. Babu SS, Praveen VK, Ajayaghosh A. *Chem. Rev.* 2014; 114: 1973-2129.
 35. Friggeri A, Feringa BL, Esch, JV. *J. Controlled Release.* 2004; 97: 241-248.
 36. Praveen VK, George SJ, Varghese R, Vijayakumar C, Ajayaghosh A. *J. Am. Chem. Soc.* 2006; 128: 7542-7550.
 37. Liu ZX, Feng Y, Yan ZC, He YM, Liu CY, Fan QH. *Chem. Mater.* 2012, 24, 3751-3757.
 38. (a) Ding AX, Yang LM, Zhang YY, Zhang GB, Kong L, Zhang XJ, Tian YP, Tao XT, Yang JX. *Chem. Eur. J.* 2014; 20: 12215-12222;
(b) Grabowski ZR, Rotkiewicz K. *Chem. Rev.* 2003; 103: 3899-4031.
 39. (a) Levitus M, Schmieder K, Ricks H, Shimizu KD, Bunz UHF, Garibay MAG. *J. Am. Chem. Soc.* 2001; 123: 4259-4265;
(b) Tong H, Hong YN, Dong YQ, Ren Y, Haussler M, Lam JWY, Wong KS, Tang BZ. *J. Phys. Chem. B.* 2007; 111: 2000-2007;
(c) Jia WB, Wang HW, Yang LM, Lu HB, Kong L, Tian YP, Tao XT, Yang JX. *J. Mater. Chem. C.* 2013; 1: 7092-7101.
 40. (a) Hong YN, Lam JWY, Tang BZ. *Chem. Commun.* 2009, 4332-4353;
(b) Liang GD, Lam JWY, Qin W, Li J, Xie N, Tang BZ. *Chem. Commun.* 2014; 50: 1725-1727;
(c) Peng Q, Yi YP, Shuai ZG, Shao JS. *J. Am. Chem. Soc.* 2007; 129: 9333-9339.